BNL-63303

CONF-960810 3--2

OPERATIONAL OBSERVATIONS OF ATYPICAL METEOROLOGICAL FEATURES USING THE WSR-88D

Jeffrey S. Tongue *
NOAA/NWS
Upton, NY

Gregory J. Lehenbauer
University of Kansas
Lawrence, KS

Paul A. Michael and Mark A. Miller
Brookhaven National Laboratory
Upton, NY

RECEIVED
AUG 12 1996
OSTI

1. INTRODUCTION

The Weather Surveillance Radar - 1988 Doppler (WSR-88D) provides invaluable information on a variety of meteorological phenomena. The high sensitivity of the WSR-88D allows for the observation of phenomena that were not observable with previous WSR's. Precipitation phase, land-sea breeze circulations and clouds are examples of phenomena that are now observable by the WSR-88D. The detection of these features has an enormous impact on forecast operations.

2. PRECIPITATION PHASE DETECTION

The delineation between frozen and liquid precipitation is routinely observed on weather radars as a band of enhanced reflectivity referred to as "the bright band." When frozen precipitation melts as it falls, a region of water-covered ice is produced. The water-covered ice is the cause of the enhanced reflectivity. Stewart and King (1990) describe the structure of the bright band.

When the radar is located on the cold (snow) side of a precipitation phase change line, the bright banding commonly appears as a line of higher reflectivity on lower radar elevation angles. When the radar site is located on the warm (rain) side, the bright band commonly appears as a circular ring of enhanced reflectivity around the radar.

A commonly occurring phenomenon in areas of precipitation phase change is precipitation banding that usually results in enhanced precipitation rates. In regions of warm advection, slantwise convection can cause banded precipitation that appears similar in reflectivity fields to bright bands associated with phase change. Discriminating between bright bands and precipitation banding in the reflectivity field data can be difficult.

The correct interpretation of banded echoes is critical to short-term forecasting. Examination of WSR-88D data from three winters along the mid-Atlantic coast has shown that 1) bright bands produce higher reflectivity values than precipitation bands, 2) bright bands propagate more slowly than precipitation bands, and 3) bright bands are typically narrower than precipitation bands. An example appears in Fig. 1.

The detection of bright bands using the WSR-88D is a critical element in the development of a snowfall accumulation algorithm. Any advanced rainfall accumulation algorithm will depend on detection of and compensation for bright banding that results in greatly overestimated rainfall amounts.

3. LAND-SEA BREEZE CIRCULATIONS

In a coastal regime, land-sea breeze circulations cause abrupt wind shifts and temperature gradients, particularly in spring. Recognizing and forecasting these circulations is critical to writing accurate forecast products. Both public temperature forecasts and aviation terminal

* *Corresponding author address:* Jeffrey S. Tongue, NOAA/NWS, 175 Brookhaven Ave., Upton, NY 11973; E-mail <jtongue@SMTPGATE.ssmc.noaa.gov>.

RB

DISCLAIMER

Portions of this document may be illegible in electronic image products. Images are produced from the best available original document.

DISCLAIMER

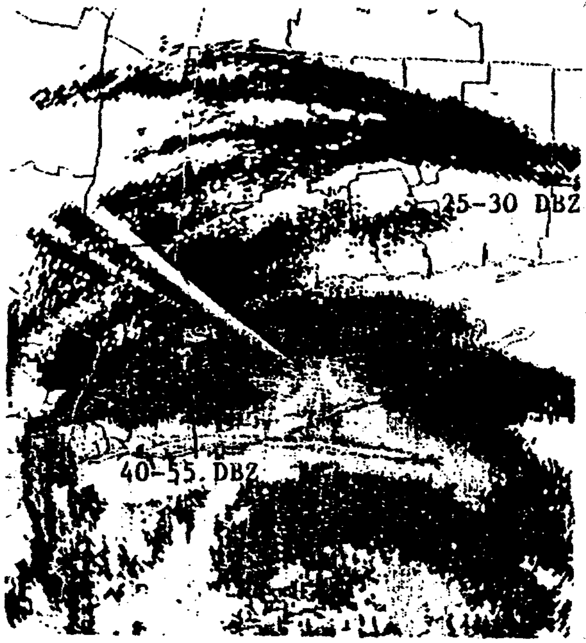

FIG. 1. Base reflectivity from the KOKX (Upton, NY) WSR-88D at 1352 UTC on 4 February 1995 at the 0.5° elevation angle. The 40-55 dBZ east-west line represents a bright band and the 25-30 dBZ east-west bands are the result of slantwise convection.

forecasts of wind direction improve dramatically when forecasters recognize land-sea breeze circulations. Aviation operations benefit from accurate anticipation of runway use changes.

The WSR-88D identifies land-sea breeze circulations as relatively narrow regions of enhanced reflectivity. A typical case in which the land-sea breeze circulation is seen in the reflectivity data from the WSR-88D is shown in Fig. 2. This is a constant altitude (0.5 km) display of reflectivity from the KOKX WSR-88D at 1800 UTC on 16 June 1995. The Interactive Radar Analysis Software (IRAS) (Priegnitz 1995) was used to produce the image. One circulation is evident over Long Island with another along the coast of Connecticut. The horizontal width of the reflectivity band varies from the limit of resolution of the radar (about 1 km) to about 5 km. It extends upward about 1 km above the surface (not shown). The reflectivity is on average 12 dBZ on Long Island west of the radar and also in Connecticut; over the south fork of Long Island, the reflectivity is 20 dBZ or higher. The reflectivity line represents the

FIG. 2. Base reflectivity from the KOKX (Upton, NY) WSR-88D at 1800 UTC 16 June 1995 at a constant altitude of 0.5 km. Range circles are labeled in kilometers.

"leading edge" of the circulation where strong baroclinicity exists and is commonly referred to as the "sea breeze front." Doppler radial velocity measurements can further define the circulations.

Initial formation of separate circulations over Long Island and Connecticut is typical. The Long Island "front" usually advances northward in the late afternoon, crossing Long Island Sound and merging with the Connecticut "front." Observations at surface-based observing stations have often confirmed the passage of the "front."

It is likely that a combination of targets causes the returns: insects (Sauvageot and Despaux 1996), refractivity variations, aerosols, suspended particulate matter, etc. When the front is over Long Island Sound, the echoes are significantly weaker. This suggests that terrestrial particulate matter has been lost and that any refractivity variation has diminished. The remaining reflectivity is likely caused by aerosols generated at the water surface.

4. DETECTION OF CLOUDS

It is possible to detect water and ice clouds with the WSR-88D. The remote observation of clouds is important to both forecasters and researchers. Of particular interest are stratus clouds and fogs, which are observable in reflectivity data. In addition, algorithms to detect parameters such as cloud thickness, cloud fraction, cloud base height and cloud top height are under development.

While precipitation typically produces reflectivity values of 20 to 60 dBZ, clouds and fog generally produce reflectivities of -30 dBZ or lower. Figure 3 shows estimates of typical reflectivity factors for stratocumulus clouds and drizzle. Table 1 shows estimates of reflectivity for several different cloud types.

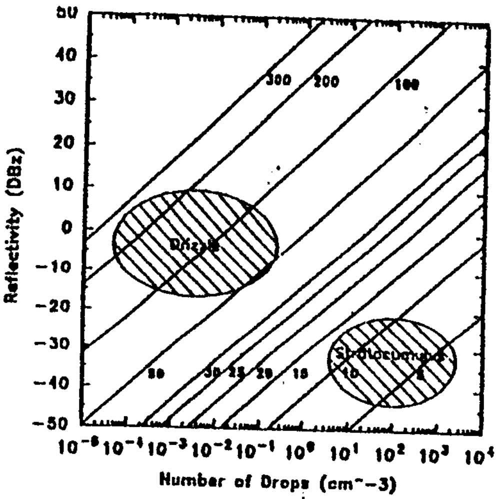

FIG. 3. Reflectivity (dBZ) versus droplet density (cm^{-3}) and droplet radius (μm). The labeled diagonal lines are isopleths of equal droplet radius and the hatched areas represent typical values for droplet number density and droplet radius taken from aircraft measurements (Miller 1994).

4.1 *Minimum Detectable Signal*

To determine if the WSR-88D is sensitive enough to detect clouds, the Minimum Detectable Signal (MDS) of the radar must be calculated from examination of the radar equation (Doviak and Zrnic 1984). The MDS for any range can be calculated if the radar constant is known. The MDS for the WSR-88D is shown in Fig. 4 for the long and short pulse widths used in the "clear air mode" volume coverage patterns 31 and 32. If clouds have an average reflectivity value of -30 dBZ, then from figure 4 it can be seen that clouds are detectable to a range of around 15 km using the 1.57 μs short pulse and to around 30 km using the 4.57 μs long pulse.

TABLE 1. Characteristics of various clouds and estimated reflectivity factors. The abbreviation "Sc" indicates stratocumulus (Miller, 1994).

CLOUD TYPE	Droplet Number Density (cm^{-3})	Droplet Radius (μm)	Liquid Water Content ($g\ kg^{-1}$)	Reflect. Factor (dBZ)
Maritime Cumulus (1)	10	15	0.4	-22
Continent. Cumulus (1)	50	5	0.4	-46
Hawaiian Orographic (1)	10	20	0.2	-16
Marine Sc Nicholls (2)	40	11.5	.1	-23
Marine Sc Albrecht (3)	40-100	9-6	.1-.15	-28,-35
Marine Sc Stop/Plate (4)	30-40	7-12	.1-.4	-22,-40
CA Rad. Fog (5)	60	9.5	.2	-25
Marine Sc Drizzle (2) 300 m	.001	100	.003	-12

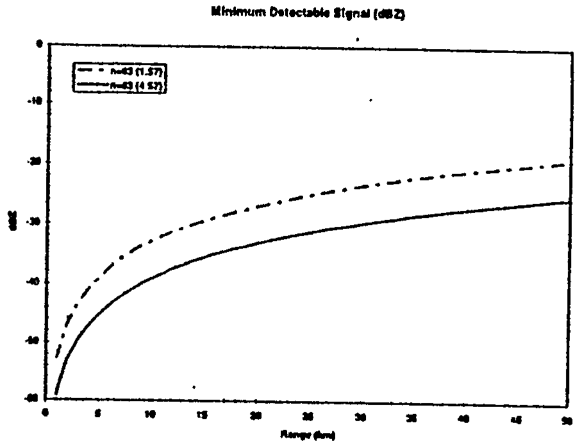

FIG. 4. Graph showing MDS for the WSR-88D's volume coverage pattern 31 (4.57 μs pulse width) and volume coverage pattern 32 (1.57 μs pulse width). The number of samples per radial is 63 for both.

4.2 *Example*

Figure 5 shows a WSR-88D reflectivity pattern from 23 February 1996. This pattern was made using an elevation angle of 1.5°, a pulse width of 4.57 μs, and 63 samples per radial (volume coverage pattern 31). On this day, low clouds were observed over the region with fog and drizzle located to the southeast of the radar. A circular pattern of reflectivities in the -24 to -32 dBZ range is observed. The outer edge of this circular area represents the loss of detectability due to receiver noise (MDS). The inner edge represents the lowest height at which echoes are observed and is comparable to cloud base height. From these data, efforts are being made to further quantify the characteristics of the cloud field in the vicinity of the radar.

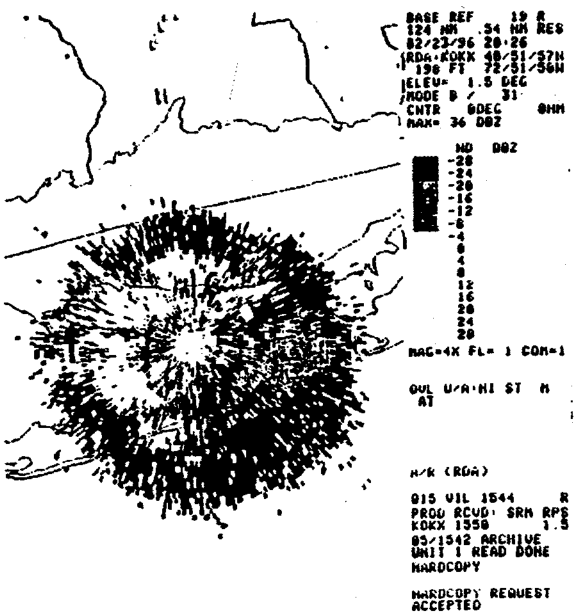

FIG. 5. Base reflectivity from the KOKX (Upton, NY) WSR-88D at 2026 UTC on 23 February 1996 for the 1.5° elevation angle. The region of -24 to -28 dBZ reflectivities depicts stratus clouds; the -8 to -23 dBZ reflectivities represents an area of drizzle.

5. CONCLUSION

The WSR-88D network is a unique meteorological observing resource. The system has proven an invaluable tool in the severe weather warning process (Bieringer and Ray 1996). However, the detection of non-severe features including clouds, land-sea breeze circulations, and precipitation phase can also affect the accuracy of both public and aviation forecasts. The WSR-88D is a powerful observing platform that can be integrated with other active and passive remote observing systems to depict a more detailed four dimensional structure of the atmosphere. Operational meteorologists should attempt to assure that the WSR-88D is used such that non-severe features are detected and integrated into the forecast process.

REFERENCES

Bieringer, P. and P.S. Ray, 1996: A comparison of tornado warning lead times with and without NEXRAD doppler radar. *Wea. Forecasting*, **11**, 47-52.

Doviak, R. J. and D. S. Zrnic, 1984: *Doppler Radar and Weather Observations*. Academic Press, Inc., 458 pp.

Miller, M. A., 1994: Surface-based remote sensing of marine boundary-layer mesoscale cloud structure during ASTEX. Ph.D. Disertation, Pennsylvania State University, 129 pp.

Priegnitz, D.L., 1995: IRAS: Software to display and analyze WSR-88D radar data. Preprints, *Eleventh International Conference on Interactive Information and Processing Systems for Meteorology, Oceanography, and Hydrology*, Boston, MA, Amer. Meteo. Soc., 197-199.

Sauvageot, H and G. Despaux, 1996: The clear-air coastal vespertine radar bands, *Bull. Amer. Meteor. Soc.*, **77**, 673-681.

Stewart, R.E. and P. King, 1990: Precipitation type transition in winter storms over southern Ontario. *J. Geophys. Res.*, **95** , 22355-22368.

6. ACKNOWLEDGMENTS

This research was partially supported by the U.S. Department of Energy under Contract No. DE-AC02-76CH00016.